J Solid State Electrochem (1997) 1: 172–179

ORIGINAL PAPER

J. Premkumar · R. Ramaraj

Electrocatalytic reduction of dioxygen at platinum particles deposited on Nafion- and clay-coated electrodes

Received: 24 January 1997 / Accepted: 14 April 1997

Abstract Nafion- and clay-coated electrodes are prepared by casting a known amount of Nafion and clay solutions on the glassy carbon electrode (GC) surface. Subsequently platinum (Pt) particles are deposited on the GC electrodes and on the Nafion- and clay-coated GC electrodes. The formation of Pt particles on the modified electrode surface is analysed by scanning electron microscope, while cyclic voltammetry provides information on the anodisation of Pt particles deposited on the GC electrodes at >0.5 V(SCE) leading to the formation of platinum oxide (PtO). The involvement of PtO on the catalysed dioxygen reduction to hydrogen peroxide is reported. Macrocyclic cobalt(III) complex is also used as the electrocatalyst. The effect of pH on the reduction of PtO and dioxygen in deaerated and oxygenated solutions is studied to understand the dioxygen reduction processes.

Key words Platinum coating · Cyclic voltammetry · Anodisation · Catalyst · Dioxygen reduction · Nafion · Clay

Introduction

Dioxygen reduction has been widely studied in both acidic and basic electrolyte solutions because of its fundamental importance in electrochemistry and also in fuel cell applications [1–6]. On the other hand, its reduction in neutral solution is interesting in the development of biosensors for dissolved oxygen in biological processes [7–9]. Metal microparticles deposited on electrode surfaces with and without polymer coatings and their resulting electrocatalytic properties have been reported [10–14]. Polymer films, such as poly(4-vinylpyridine) and polypyrrole, enhance the stability and dispersity of the embedded Pt particles on GC electrodes. Use of deposited metal particles for both hydrogen evolution and oxygen reduction have been investigated [12–17]. In the present study, the deposition of Pt particles in Nafion and clay films and their electrocatalytic properties were studied. The mobility of dioxygen within the Nafion film was reported to be higher than in water [18]. The Pt particles deposited on GC electrodes coated with Nafion and clay exhibited better catalytic activity for dioxygen reduction than Pt particles deposited on bare GC electrode.

J. Premkumar · R. Ramaraj (✉)
School of Chemistry, Madurai Kamaraj University, Madurai-625 021, India

Experimental

GC electrode was used as the substrate to prepare Nafion- and clay-coated electrodes. The GC electrode surface was polished to a mirror finish with a 0.3-μm alumina powder [19] followed by thorough washing with distilled water in an ultrasonic bath. All other chemicals were Analar grade and used as received. A 5% Nafion (Nf) solution (Aldrich, EW 1100, dissolved in a mixture of lower aliphatic alcohol and water) was diluted to 0.5% with ethanol. A 0.1% bentonite clay (BT) solution (Aldrich) was prepared with distilled water. Chloroplatinic acid (H_2PtCl_6) was purchased from Aldrich. The macrocyclic cobalt(III) complex, $[Co(cyclam)(H_2O)_2]^{3+}$ (cyclam = 1, 4, 8, 11 tetraazacyclotetradecane), referred to below as "Co(III) complex", was prepared according to the literature procedure [20]. An all-glass apparatus was used to prepare doubly distilled water.

The Nafion- or clay-coated GC (referred to below as GC/Nf or GC/BT) electrode was prepared by placing a known volume of 0.5% Nafion solution or 0.1% bentonite clay colloid onto the surface of the GC electrode (0.07 cm^2) with the aid of a micropipette (Hamilton) and dried at room temperature for 10–60 min. Subsequently, the GC/Nf and GC/BT electrodes were washed and kept in distilled water for 30 min. The thickness of the Nafion and clay films were calculated as 1.7 and 1.6 μm respectively using a density of 1.58 g/cm^3 for Nafion [21] and 1.77 g/cm^3 for clay [22]. The electrodes (GC, GC/Nf and GC/BT) were dipped in a mixture of deaerated 1 M H_2PtCl_6 and 1 M $HClO_4$ solution for 5 min followed by continuous scanning of the electrode between the potential 1.0 and −0.1 V(SCE) to deposit Pt particles onto the GC, GC/Nf and GC/BT electrodes. The electrodes were washed and dipped in distilled water and used for electrochemical experiments (the electrodes are referred to below as GC/Pt, GC/Nf/Pt and GC/BT/Pt). Electrochemical measurements were performed on an

EG&G PAR model 273A Potentiostat/Galvanostat equipped with REO151 X–Y recorder. A three-electrode cell (Pt-particle-deposited GC or GC/Nf or GC/BT as working electrode, Pt plate as counter electrode and a saturated calomel electrode (SCE) as reference electrode) was used to record cyclic voltammograms. Pure grade nitrogen and oxygen gases were used to degas and oxygenate the experimental solutions respectively. All potentials in the text were referred to SCE.

The dioxygen reduction experiment was carried out under applied potential condition using anodised (at 1.3 V) Pt particles deposited onto a GC electrode by dipping in oxygenated 0.1 M H_2SO_4 solution. Oxygen gas was continuously bubbled into the cell solution to maintain an adequate concentration of oxygen. Hydrogen peroxide was analysed by titrimetric and spectrophotometric (JASCO UV-VIS spectrophotometer) methods [23, 24]. For pH variation experiments, the pH was maintained in the experimental solution by using standard buffer solutions [25]. The pHs of the standard buffer solutions were checked with a pH meter (Philips PR 9404). The surface morphology of the Pt-particles-deposited Nf and BT films were examined by scanning electron microscope (SEM) (Hitachi S-450). ITO (indium tin oxide)-coated glass plates were used as substrates for recording the scanning electron micrographs.

Results and discussion

Deposition of Pt particles

The continuous cyclic voltammograms recorded between 1.0 and −0.1 V at a scan rate of 10 mV/s for GC, GC/Nf and GC/BT in a mixture of 1 M H_2PtCl_6 and 1 M $HClO_4$ are shown in Fig. 1. In the first scan the four-electron reduction of Pt(IV) to Pt(0) occurred at 0.1 V [26]. In the subsequent cycles, the peak current observed at 0.1 V disappeared completely and a new irreversible reduction peak was observed around 0.3 V. This indicates that the deposition of Pt particles occurred in the first cycle and the Pt underwent oxidation at >0.5 V in the oxidative scan between −0.1 and 1.0 V.

In an aqueous acidic solution (0.1 M H_2SO_4, pH 0.7), when the potential exceeded >0.4 V in the scan from −0.1 to 1.0 V, the Pt particles deposited on the GC electrode were oxidised to form platinum oxide (PtO). The reported formation of PtO at a plain Pt electrode surface and its reduction back to Pt take place according to Eqs. 1 and 2 [27]. Electrochemical and optical

$$Pt + H_2O \longrightarrow PtO + 2H^+ + 2e^- \quad (1)$$

$$PtO + 2e^- + 2H^+ \longrightarrow Pt + H_2O \quad (2)$$

studies of the anodised Pt electrode revealed that the quantity of bound oxygen (as PtO) increased with increase of the positive potential, exceeding monolayer amounts [27–31].

SEM analysis

The SEM photographs of the Pt particles deposited onto ITO and Nafion- and clay-coated ITO electrodes are shown in Fig. 2. The dispersed Pt particles appear as dark spots in the photographs and appear to be homogeneously dispersed, adhering to the electrode surface. The SEM photographs indicate a particle size distribution of Pt particles (~80–100 nm dia). In the present investigation, at Nafion and clay films (thicknesses of 1.7 μm and 1.6 μm respectively), the Pt particle size was rather bigger and visually distinguishable (Fig. 2). In addition, scanning electron micrographs showed that the Pt particles were finely dispersed on the polymer and clay films.

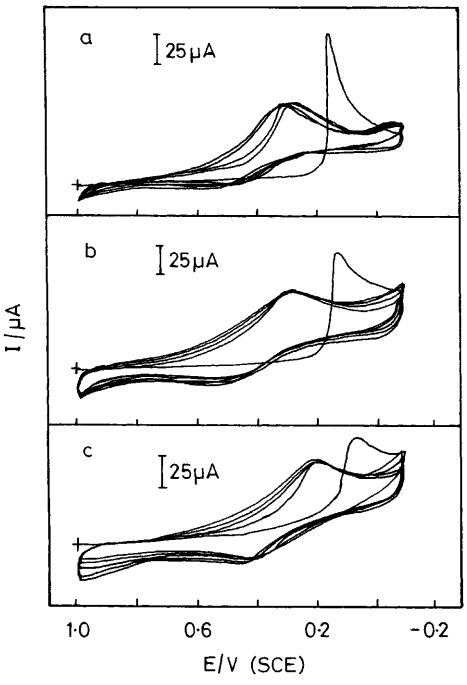

Fig. 1 Continuous cyclic voltammograms of **a** GC, **b** GC/Nf and **c** GC/BT electrodes in deaerated 1 M H_2PtCl_6 and 1 M $HClO_4$. Scan rate 10 mV/s

Electrochemical reduction of PtO at PtO-covered Pt particles

Typical cyclic voltammograms obtained for GC, GC/Pt, GC/Nf/Pt and GC/BT/Pt electrodes in deaerated 0.1 M H_2SO_4 solution are shown in Figs. 3–6. All the electrode systems showed an irreversible reduction peak at 0.4 V, and this was ascribed to the reduction of PtO to Pt (Eq. 2). On raising the positive potential range from 0.6 to 1.3 V, the cathodic peak current increased and reached a maximum due to the greater amount of formation and reduction of PtO in deaerated 0.1 M H_2SO_4 (Eqs. 1 and 2). The anodisation of Pt particles at 1.3 V over different times was studied, and it was found that the PtO reduction current remained constant after 3 min of anodisation. The reduction peak at 0.4 V for PtO-covered Pt particles deposited on the GC electrode was not observed for bare GC electrode. In the present investigation, the Pt-particles-deposited electrode be-

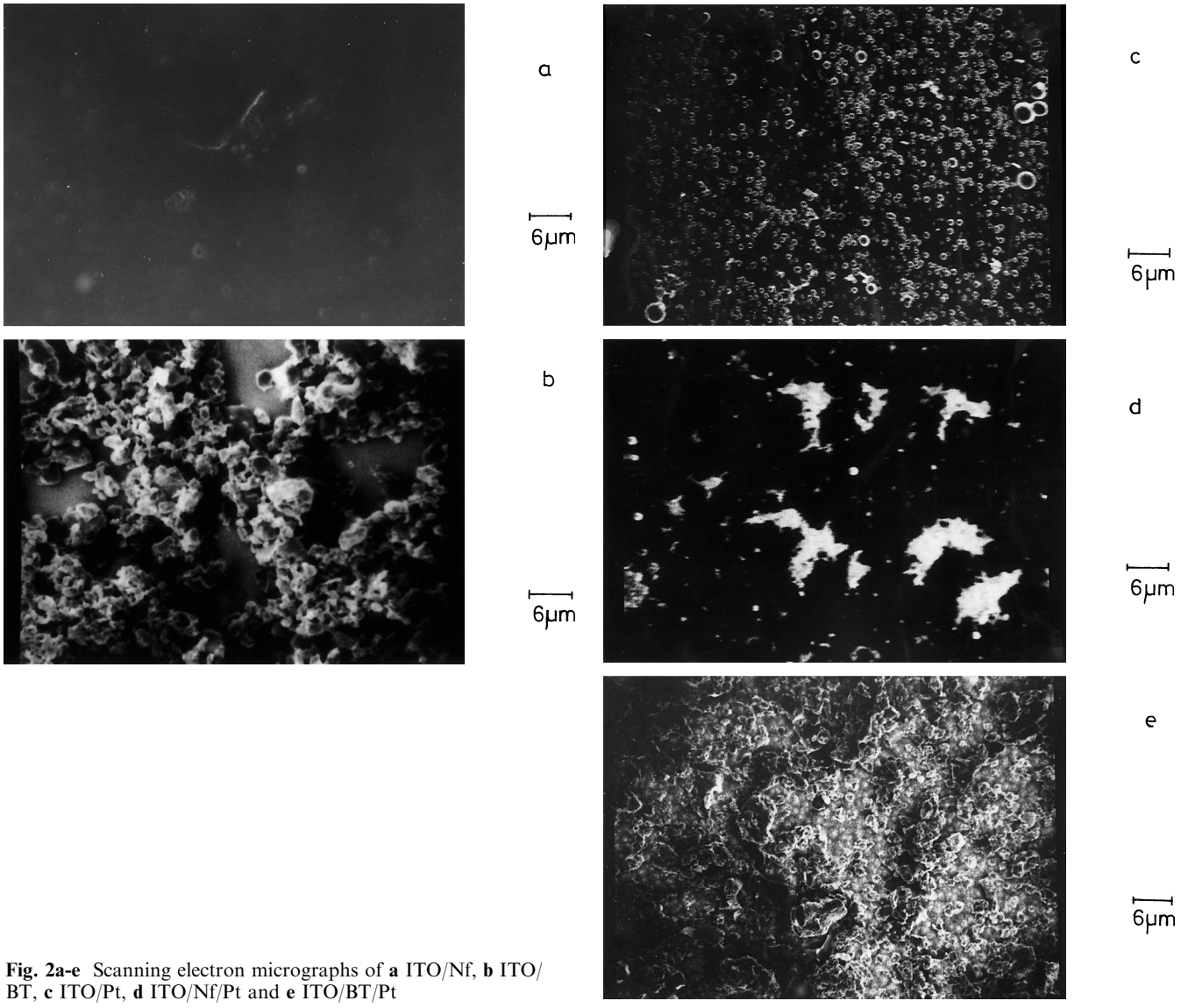

Fig. 2a-e Scanning electron micrographs of **a** ITO/Nf, **b** ITO/BT, **c** ITO/Pt, **d** ITO/Nf/Pt and **e** ITO/BT/Pt

haved very similarly to the plain Pt electrode. Reduction of surface oxide layer to the corresponding metal [32] enables the reestablishment of the initial state of the metal surface between experiments. The oxide film can be grown reproducibly.

The position and magnitude of the PtO reduction current showed that a similar dispersion of Pt particle coating could be obtained in each run. Increasing the amount of Pt particle deposited in the film coating by increasing the film thickness of Nafion and clay films did not bring about further increase in the PtO reduction current. The reduction peak potential of PtO in deaerated buffer solution (pH 1 to 8) using PtO-covered Pt-particle-coated electrode showed a pH dependence due to the electron-proton coupling nature of the net redox reaction (Eq. 2). The plots of the reduction peak potential of PtO vs pH for GC/Pt, GC/Nf/Pt and GC/BT/Pt electrodes in the deaerated condition are shown in Fig. 7. A less pronounced break was observed in the plot at pH 3–4 (Fig. 7), which arises because of the proton involved in the reduction of PtO to H_2O (Eq. 2). The PtO reduction to water involved two electrons and two protons. The plots showed a shift in the reduction peak of PtO and a pH dependence of approximately 60 mV/pH (Fig. 7).

Electrochemical reduction of dioxygen at PtO-covered Pt particles

Cyclic voltammograms recorded for GC and Pt-particle-deposited GC electrodes (GC/Pt, GC/Nf/Pt and GC/BT/Pt) in oxygenated 0.1 M H_2SO_4 at various potential regions are shown in Figs. 3–6. An irreversible reduction peak with increased cathodic peak current was observed at 0.4 V. When the positive potential range was increased from 0.6 to 1.3 V an increase in the cathodic peak current was observed at 0.4 V. These

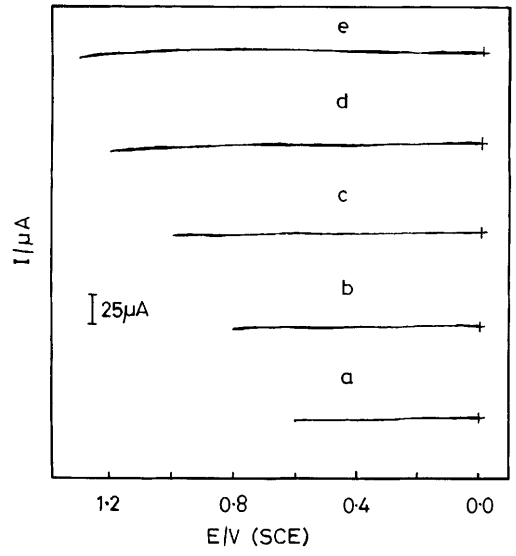

Fig. 3a–e Cyclic voltammograms of GC, GC/Nf and GC/BT electrodes in deaerated and oxygenated 0.1 M H_2SO_4 at different potential regions **a** 0.0–0.6 V, **b** 0.0–0.8 V, **c** 0.0–1.0 V, **d** 0.0–1.2 V and **e** 0.0–1.3 V. Scan rate 10 mV/s

observations showed that the PtO formed at the Pt-particle-deposited electrode was involved in the dioxygen reduction process. The partial reduction product was found to be hydrogen peroxide. This indicates that the dioxygen undergoes two-electron reduction to the hydrogen peroxide stage at PtO-covered Pt particle

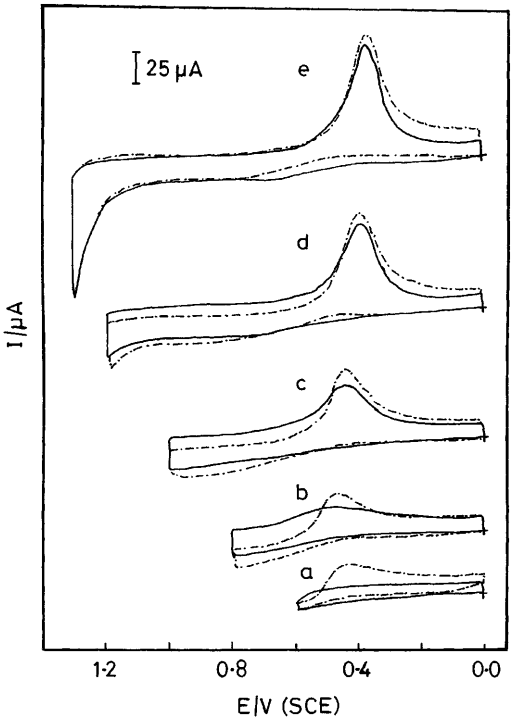

Fig. 5a–e Cyclic voltammograms of GC/Nf/Pt electrode in deaerated (——) and oxygenated (– · – · –) 0.1 M H_2SO_4 at different potential regions. **a** 0.0–0.6 V, **b** 0.0–0.8 V, **c** 0.0–1.0 V, **d** 0.0–1.2 V and **e** 0.0–1.3 V. Scan rate 10 mV/s

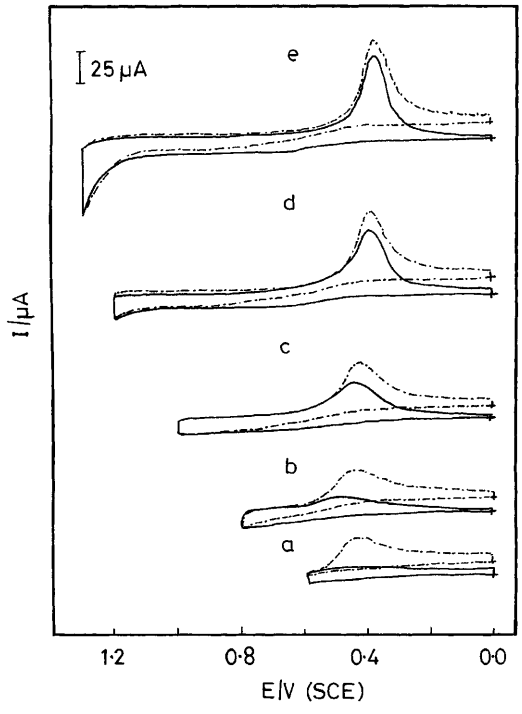

Fig. 4a–e Cyclic voltammograms of GC/Pt electrode in deaerated (——) and oxygenated (– · – · –) 0.1 M H_2SO_4 at different potential regions: **a** 0.0–0.6 V, **b** 0.0–0.8 V, **c** 0.0–1.0 V, **d** 0.0–1.2 V and **e** 0.0–1.3 V. Scan rate 10 mV/s

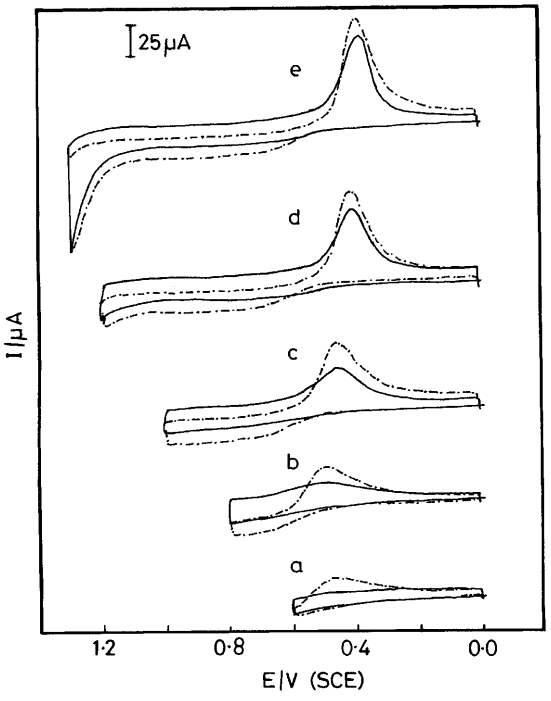

Fig. 6a–e Cyclic voltammorgams of GC/BT/Pt electrode in deaerated (——) and oxygenated (– · – · –) 0.1 M H_2SO_4 at different potential regions: **a** 0.0–0.6 V, **b** 0.0–0.8 V, **c** 0.0–1.0 V, **d** 0.0–1.2 V and **e** 0.0–1.3 V. Scan rate 10 mV/s

deposited electrodes in addition to its four-electron reduction to water (Eqs. 3 and 4). The dioxygen reduction reaction on Pt proceeded through a pathway involving the adsorption of O–O and decomposition of the O–O bond [33]. In the present work, the PtO-covered Pt electrode favoured the partial desorption of the two-electron reduction product hydrogen peroxide into the solution. The adsorbed hydrogen peroxide was much more readily desorbed from the site on PtO than from the adsorption site involved in the four-electron reduction process at Pt.

$$O_2 + 2\,e^- + 2\,H^+ \xrightarrow{PtO} H_2O_2 \quad (3)$$

$$O_2 + 4\,e^- + 4\,H^+ \xrightarrow{Pt/PtO} 2\,H_2O \quad (4)$$

Figs. 3–6 show the cyclic voltammograms obtained for the reduction of dioxygen in the absence and presence of Pt particles at GC, GC/Nf and GC/BT electrodes. The dioxygen reduction commences at more positive potentials and the current rises more steeply. It may be noted that the position of the catalysed dioxygen reduction wave is coupled with the reduction of PtO.

The dioxygen reduction potential at Pt-particle-deposited electrodes depended upon the degree of "activation" of the Pt particle on the GC surface. At a bare GC electrode, the reduction occurred at ca. −0.5 V(SCE) in 0.1 M H_2SO_4 [34]. When Pt particles were deposited on GC electrode, the dioxygen reduction potential was shifted to a higher positive potential (0.4 V). Nafion and clay films were found to be good support materials for Pt particle deposition. It seems likely that the PtO reduction potential at which dioxygen reduction occurred can be used to judge the state of "activity" of the PtO-covered Pt particle catalyst dispersed in the Nafion and clay films. The schematic view of the dioxygen reduction mechanism at PtO- and Pt-particle catalyst-deposited electrodes are shown in Fig. 8.

The controlled potential electrolysis experiment with anodised GC/Pt, GC/Nf/Pt and GC/BT/Pt electrodes showed a maximum yield of hydrogen peroxide at 0.4 V. At an applied potential of 0.4 V, the yield of hydrogen peroxide was measured using the modified electrodes at different time intervals, and the results are shown in Fig. 9. At an applied potential of 0.4 V for 30 min using anodised (> 1.0 V) GC, GC/Pt, GC/Nf/Pt and GC/BT/Pt electrodes, the yields of hydrogen peroxide were observed as 0.0, 0.031, 0.053 and 0.045 μmoles respectively. The analysis of the charge accumulated at the dioxygen reduction potential (0.4 V) showed that around 40% of the conversion of dioxygen to hydrogen peroxide was occurring at PtO-covered Pt-deposited electrodes. At longer times (30 min), the PtO might undergo reduction to Pt and 0.4 V in addition to the PtO-catalysed dioxygen reduction, and the yield of formation of hydrogen peroxide reached a maximum. When the Pt particles at the modified electrodes were

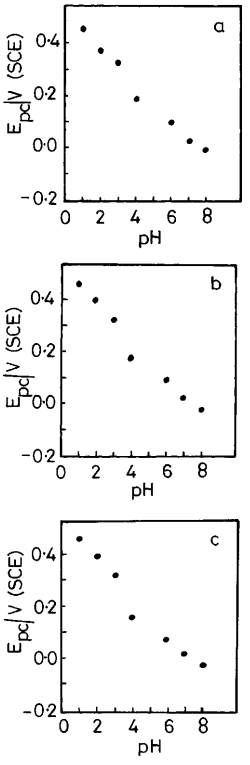

Fig. 7a–c PtO reduction peak potential (E_{pc}) as a function of pH observed in deaerated buffer solutions using PtO-covered Pt-particle-modified electrodes: **a** GC/Pt, **b** GC/Nf/Pt and **c** GC/BT/Pt electrodes

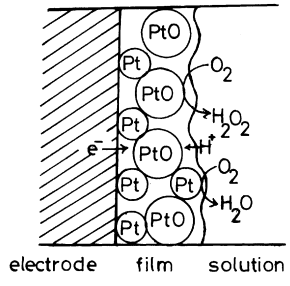

Fig. 8 Schematic view of mechanism of dioxygen reduction at PtO-covered Pt-particle-deposited GC electrodes

again anodised, the PtO-catalysed reduction of dioxygen to hydrogen peroxide was observed.

Under deaerated conditions, the PtO formed on Pt-particle-deposited GC, GC/Nf and GC/BT electrodes was reduced at an applied potential of 0 V for 15 min (Eq. 2), and the resulting GC/Pt, GC/Nf/Pt and GC/BT/Pt electrodes were used for dioxygen reduction at an applied potential of 0.4 V. In this case, dioxygen reduction to hydrogen peroxide was not observed. This observation establishes the involvement of PtO formed on the Pt-particle-deposited electrode in the two-electron reduction of dioxygen to hydrogen peroxide. To support the above observation, the pH dependence of dioxygen reduction was examined over the pH range

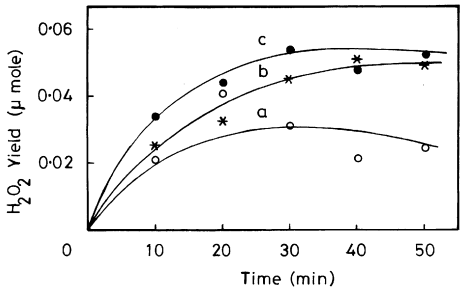

Fig. 9 Hydrogen peroxide yield observed at an applied potential of 0.4 V(SCE) using anodised **a** GC/Pt, **b** GC/Nf/Pt and **c** GC/BT/Pt electrodes dipped in oxygenated 0.1 M H_2SO_4

1–8 using standard buffer solutions. The reduction potential observed for dioxygen reduction at PtO-covered Pt-particle-deposited electrodes in oxygenated solution showed pH dependence due to the electron-proton-coupled net reduction reaction (Eq. 5). The effect of pH on the catalytic

$$O_2 + 2\,H^+ \xrightarrow{PtO} H_2O_2 \qquad (5)$$

reduction of dioxygen at the modified electrodes was studied, and the plots of dioxygen reduction potential vs pH at PtO-covered Pt-particle-deposited electrode for GC/Pt, GC/Nf/Pt and GC/BT/Pt electrodes are shown in Fig. 10. A distinct break was observed in the plots at pH 4–5. It is interesting to note that the break occurred in the pH region between 4 and 5, which is the same as the pK of hydrogen peroxide. The break points observed for GC/Nf/Pt and GC/BT/Pt electrodes are noticeably greater than that at the GC/Pt electrode (Fig. 10). This may be due to the microenvironment provided by the film (Nafion and clay), which would tend to stabilise the reduction process. The partial reduction of dioxygen to hydrogen peroxide at PtO-covered Pt-particle-modified electrodes involves two electrons and two protons. The plots shown in Fig. 10 showed a shift in the reduction peak of dioxygen and a pH dependence of approximately 60 mV/pH. The results described above suggest a general method for preparing metal and metal oxide particle catalysts in combination with polymer/clay films to extend the range of their electrocatalytic applications.

Electrocatalytic reduction of dioxygen at PtO-covered Pt-particle-deposited electrodes in the presence of Co(III) complex

Figures 11 and 12 show the cyclic voltammograms of GC, GC/Pt, GC/Nf/Pt and GC/BT/Pt in the presence of 1 mM Co(III) complex in deaerated and oxygenated 0.1 M H_2SO_4. In the absence of Pt particle, the GC electrode did not show electrocatalytic activity in the potential region between 1.0 and 0 V (Fig. 11), while in the presence of Co(III) complex in solution the Pt particle deposited onto GC or Nafion-and clay-coated GC electrodes showed a reduction peak at 0.4 V (Figs. 11 and 12) which is similar to the one observed for the same electrodes in the absence of Co(III) complex. The Co(III) complex is known to reduce dioxygen to hydrogen peroxide electrocatalytically [35] and photocatalytically [36]. The Co(III) complex showed a clear reversible one-electron redox wave [35]. The electrochemically reduced Co(II) complex reacts with dioxygen to form a Co(II)-oxygen adduct, Co(III)-O_2H, at pH 1, and this undergoes further reduction to produce hydrogen peroxide and Co(II) complex.

Recently, Pt particles have been deposited onto GC, GC/Nf and PA-coated GC electrode [12, 26] and used for dioxygen reduction. Dong and Qiu [26] reported that the cobalt porphyrin electrocatalysed the reduction of dioxygen at GC/Pt and GC/Nf/Pt electrodes around 0.3 V(SCE) in 0.05 M H_2SO_4. In the absence of cobalt porphyrin, GC/Pt and GC/Nf/Pt electrodes showed a dioxygen reduction peak around 0.3 V(SCE) [26] which is similar to the peak observed in our work (Figs. 11 and 12). In the absence of dioxygen in solution (deaerated condition), Dong and Qiu [26] observed a less intense reduction peak around 0.3 V(SCE) and, in the presence of dioxygen, a much less intense reduction peak at the

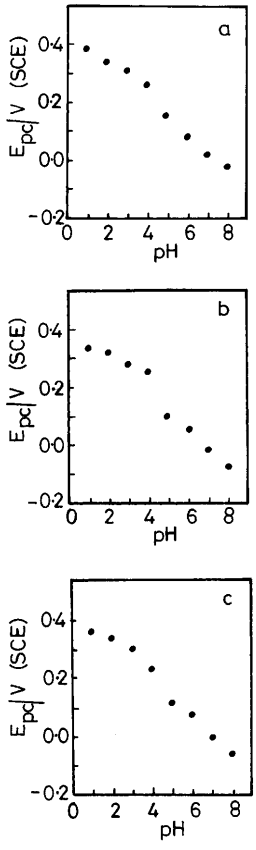

Fig. 10a–c Catalysed dioxygen reduction peak potential (E_{pc}) as a function of pH observed in oxygenated buffer solutions using PtO-covered Pt-particle-modified electrodes: **a** GC/Pt, **b** GC/Nf/Pt and **c** GC/BT/Pt electrodes

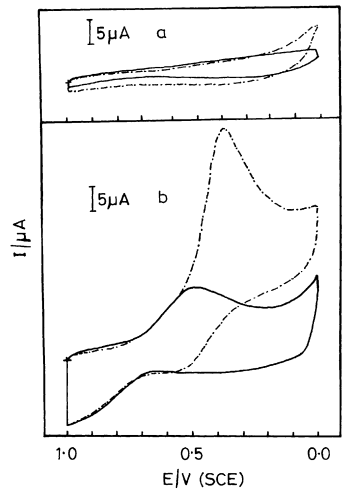

Fig. 11a,b Cyclic voltammograms of **a** GC and **b** GC/Pt electrodes in deaerated (——) and oxygenated (– · – · –) 1 mM [Co(cyclam) $(H_2O)_2]^{3+}$ and 0.1 M H_2SO_4

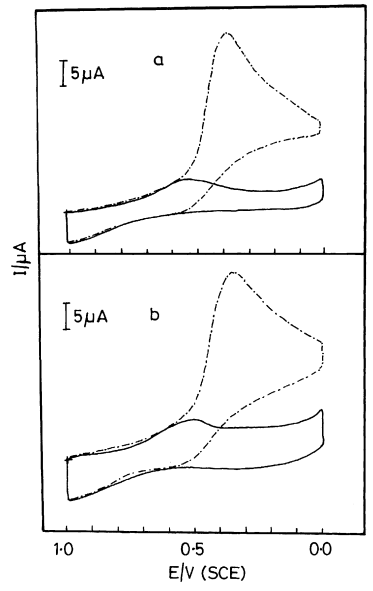

Fig. 12a,b Cyclic voltammogram of **a** GC/Nf/Pt and **b** GC/BT/Pt electrodes in deaerated (——) and oxygenated (– · – · –) 1 mM [Co(cyclam) $(H_2O)_2]^{3+}$ and 0.1 M H_2SO_4

same potential. However, they ignored this. In the oxidative scan from −0.2 to 0.8 V(SCE), the Pt particle oxidation leads to the formation of PtO, as is evident from the oxidation current starting from 0.4 V(SCE) [26]. Cui and Lee [12] reported a very similar observation for dioxygen reduction using a GC/PA/Pt electrode at pH 5.85. In the present work, the PtO reduction was observed around 0 V at pH 6.0, which is similar to the reported value of 0 V(SCE) reported by Cui and Lee [12]. From our work, we understood that the catalytic reduction wave around 0.3 V (SCE) at pH 1 reported by Dong and Qiu [26] and around 0 V(SCE) at pH 5.85 by reported Cui and Lee [12] is due to the reduction of PtO and electrocatalysed reduction of dioxygen by PtO-covered Pt particle. In the cyclic voltammetry study, if one stops the oxidative scanning potential below 0.4 V(SCE), the formation of PtO can be avoided, showing electrocatalytic reduction of dioxygen by Pt particle as reported by Bose and Rajeshwar [14] using a GC/polypyrrole/Pt electrode and Liu and by Anson [11] using a graphite carbon/Nf/Pt/$[Ru(NH_3)_6]^{3+}$ electrode. We conclude from our work that the oxidative scanning between 0 and 0.4 V(SCE) will keep Pt particle as Pt and the increase of the positive potential region above 0.4 V(SCE) will lead to the formation of PtO on Pt particle (Fig. 11). The formation of PtO electrocatalyses dioxygen reduction at 0.4 V, and the introduction of metal complex catalyst did not show a marked effect in this potential region since the metal complex catalyses dioxygen reduction at a slightly more negative potential [0 V(SCE)] [35] than in the case of PtO.

Acknowledgements The financial support from the Department of Science and Technology and the Council of Scientific and Industrial Research in the form of projects to R.R. and a Senior Research Fellowship to J.P. is gratefully acknowledged. The authors thank Prof. G. Kulandaivelu for his help in recording the scanning electron micrographs.

References

1. Collman JP, Denisevich P, Konai Y, Marrocco M, Koval C, Anson FC (1980) J Am Chem Soc 102: 6027
2. Niederhoffer EC, Timmons JH, Martell AE (1984) Chem Rev 84: 137
3. Sawyer D T (1991) Oxygen chemistry. Oxford University Press, New York
4. Appleby AJ (1993) J Electroanal Chem 357: 117 and references cited therein
5. Kinoshita K (1992) Electrochemical oxygen technology. Wiley, New York
6 Srinivasan S, Bockris JO'M (1969) Fuel cells: their electrochemistry. Mc Graw-Hill, New York
7. Delahay P (1950) J Electroanal Chem 97: 198
8. Brandt ES (1983) J Electroanal Chem 150: 97
9. Gouerec P, Bilou A, Contamin O, Scarbeck G, Savy M, Barbe JM, Guilard R (1995) J. Electroanal Chem 398: 67
10. Rubinstein I, Bard AJ (1980) J Am Chem Soc 102: 6641
11. Liu H, Anson FC (1983) J Electroanal Chem 158: 181
12. Cui CQ, Lee JY (1994) J Electroanal Chem 367: 205
13. Weisshaar DE, Kuwana T (1984) J Electroanal Chem 163: 395
14. Bose CSC, Rajeshwar K (1992) J Electroanal Chem 333: 235
15. Holdcroft S, Funt BL (1988) J Electroanal Chem 240: 89
16. Kost KM, Bartak DE, Kazee B, Kuwana T (1990) Anal Chem 62: 151
17. Yang Y, Zhou Y (1995) J Electroanal Chem 397: 271
18. Ogumi Z, Kuroe T, Takehara Z (1985) J Electrochem Soc 132: 2601
19. Matsue T, Suda M, Uchida I (1987) J Electroanal Chem 234: 163
20. Bosnich B, Poon CK, Tobe ML (1965) Inorg Chem 4:1102
21. Martin CR, Rubinstein I, Bard AJ (1982) J Am Chem Soc 104: 4817
22. Grim RE (1969) Clay minerology. Mc Graw-Hill, New York
23. Vogel AI (1975) Tex-book of quantitative inorganic analysis, 3rd ed. Longman, pp 295
24. Heckman RA, Espenson JH (1979) Inorg Chem 18: 37

25. Dean JA, (1972) Lange's Handbook of chemistry 12th edn. Mc Graw-Hill. New York
26. Dong S, Qiu Q (1991) J Electroanal Chem 314: 223
27. Vetter KJ, Schultze JW (1972) J Electroanal Chem 34: 131
28. Bockris JO'M, Genshaw MA, Reddy AKN (1964) J Electroanal Chem 8: 406
29. Reddy AKN, Genshaw MA, Bockris JO'M (1968) J Chem Phys 48: 671
30. Parsons R, Visscher WM (1972) J Electroanal Chem 36: 329
31. Angerstein-Kozlowska H, Conway BE, Sharp WBA (1973) J Electroanal Chem 43: 9
32. Rudge AJ, Peter LM, Hards GA, Potter RA (1994) J Electroanal Chem 366: 253
33. Yeager E (1984) Electrochim Acta 29: 1527
34. Premkumar J, Ramaraj R (1996) J Appl Electrochem 26: 763
35. Geigar T, Anson FC (1981) J Am Chem Soc 103: 7489
36. Premkumar J, Ramaraj R (1996) J Chem Soc Chem Commun 761